ЖЭТФ, 2012, том 141, вып. 6, стр. 1071–1083

BLACK HOLE EVAPORATION IN A NONCOMMUTATIVE CHARGED VAIDYA MODEL

*M. Sharif**, *W. Javed*

Department of Mathematics, University of the Punjab
54590, Lahore, Pakistan

Received October 25, 2011

We study the black hole evaporation and Hawking radiation for a noncommutative charged Vaidya black hole. For this purpose, we determine a spherically symmetric charged Vaidya model and then formulate a noncommutative Reissner–Nordström-like solution of this model, which leads to an exact $(t-r)$-dependent metric. The behavior of the temporal component of this metric and the corresponding Hawking temperature are investigated. The results are shown in the form of graphs. Further, we examine the tunneling process of charged massive particles through the quantum horizon. We find that the tunneling amplitude is modified due to noncommutativity. Also, it turns out that the black hole evaporates completely in the limits of large time and horizon radius. The effect of charge is to reduce the temperature from a maximum value to zero. We note that the final stage of black hole evaporation is a naked singularity.

1. INTRODUCTION

The classic concept of a smooth spacetime manifold breaks down at short distances. Noncommutative geometry offers an impressive framework to investigate the short-distance spacetime dynamics. In this framework, a universal minimal length scale $\sqrt{\sigma}$ exists (equivalent to the Planck length). In general relativity, the effects of the noncommutativity can be taken into account by keeping the standard form of the Einstein tensor and using the altered form of the energy–momentum tensor in the field equations. This involves a distribution of point-like structures in favor of smeared objects[1]. Noncommutative black holes (BH) require an appropriate framework in which the noncommutativity corresponds to the general relativity.

Black hole evaporation leads to comprehensive and straightforward predictions for the distribution of emitted particles. However, its final phase is unsatisfactory and cannot be resolved due to the semiclassical representation of the Hawking process. Black hole evaporation can be explored in curved spacetime by quantum field theory but the BH itself is described by a classical background geometry. On the other hand, the final stage of BH decay requires quantum gravity corrections while the semiclassical model is incapable to discuss evaporation. Noncommutative quantum field theory (based on the coordinate coherent states) treats the short-distance behavior of point-like structures, where mass and charge are distributed over a region of size $\sqrt{\sigma}$.

Hawking [1] suggested that the radiation spectrum of an evaporating BH is just like a purely thermal black-body spectrum, i.e., the BH can radiate thermally. Consequently, a misconception [2] was developed with respect to the information loss from a BH, leading to the nonunitary of the quantum evolution[2]. Accordingly, when a BH evaporates completely, all the information related to matter that has fallen inside the BH is lost. Gibbons and Hawking [3] proposed a formulation to visualize radiation as tunneling of charged particles. In this formulation, radiation corresponds to electron–positron pair creation in a constant electric field, with the energy of a particle changing sign as it

*E-mail: msharif.math@pu.edu.pk

[1] An object constructed by means of a generalized function $\rho(t,r)$ is smeared in space and is known as a smeared object. These objects are nonlocal. Smearing cannot change the physical nature of the object but the spatial structure of the object is changed, being smeared in a certain region determined by $\sqrt{\sigma}$.

[2] Nonunitary quantum evolution is one of the interpretations of the information paradox to modify quantum mechanics. In a unitary evolution, the entropy is constant with the usual S-matrix, whereas it is not constant in a nonunitary quantum evolution.

crosses the horizon. The total energy of a pair created just inside or outside the horizon is zero when one member of the pair tunnels to the opposite side. Parikh and Wilczek [4] derived Hawking radiation as a tunneling through the quantum horizon on the basis of null geodesics. In this framework, the BH radiation spectrum corrected due to back-reaction effects is obtained. This tunneling process shows that the extended radiation spectrum is not exactly thermal yielding a unitary quantum evolution.

There are two different semiclassical tunneling methods to calculate the tunneling amplitude, which lead to the Hawking temperature. The first method, called the null geodesic method, gives the same temperature as the Hawking temperature. The second method, called the canonically invariant tunneling, leads to a canonically invariant tunneling amplitude and hence the corresponding temperature which is higher than the Hawking temperature by a factor of 2 [5]. It was argued in [6] that a particular coordinate transformation resolves this problem in the semiclassical picture.

Black hole evaporation spectra in the Einstein–dilaton–Gauss–Bonnet four dimensional string gravity model was discussed in [7] using the radial null geodesic method. It was shown that BHs should not disappear and become relics at the end of the evaporation process. The authors of [7] numerically investigated the possibility of experimental detection of such remnant BHs and discussed the mass loss rate in analytic form. These primordial BH relics could form a part of the nonbaryonic dark matter in our universe.

Various noncommutative models in terms of coordinate coherent states that satisfy the Lorentz invariance, unitarity, and UV finiteness of quantum field theory were found in [8]. A generalized noncommutative metric that does not allow a BH to decay below a minimal nonzero mass M_0, i. e., the BH remnant mass, was derived in [9]. The effects of noncommutative BHs have been studied [10, 11] and consistent results were found. The evaporation process stops when a BH approaches a Planck-size remnant with zero temperature. Also, it does not diverge but rather reaches a maximum value before shrinking to the absolute zero temperature, which is an intrinsic property of the manifold. Some other authors [12] also explored information loss problem during BH evaporation.

Quantum corrections to the thermodynamical quantities for a Bardeen charged regular BH were investigated in [13] using the quantum tunneling approach over semiclassical approximations. In a recent work [14], the effects of noncommutativity on the thermodynamics of this BH were discussed. The tunneling of massive particles through the quantum horizon of the noncommutative Schwarzschild BH was analyzed in [15] and the modified Hawking radiation, thermodynamical quantities, and emission rate was derived. Stable BH remnants and the information loss issues were also discussed there. The effects of smeared mass were studied in [17] with the conclusion that information might be saved by a stable BH remnant during the evaporation process. In [17], this work was extended to a noncommutative Reissner–Nordström (RN) BH and the emission rate consistent with a unitary theory was determined. The same author [18] also formulated a noncommutative Schwarzschild-like metric for a Vaidya solution and analyzed three possible causal structures of the BH initial and remnant mass. He also studied the tunneling of charged particles through the quantum horizon of the Schwarzschild-like Vaidya BH and evaluated the corresponding entropy.

The purpose of this paper is two-fold. First, we formulate a noncommutative RN-like solution of the spherically symmetric charged Vaidya model. Second, we investigate some of its features. In particular, we explore the BH evaporation and Parikh–Wilczek tunneling process. The paper is organized as follows. In Sec. 2, we solve the coupled field equations for the spherically symmetric charged Vaidya model. The effect of the noncommutative form of this model is investigated in the framework of coordinate coherent states in Sec. 3. Here, an exact $(t-r)$-dependent RN-like BH solution is obtained. In Sec. 4, we find the behavior of the temporal component of this solution and also discuss the BH evaporation in the limits of large time and charge. In Sec. 5, we study the Parikh–Wilczek tunneling for such a Vaidya solution and the Hawking temperature in the presence of a charge. The tunneling amplitude at which massless particles tunnel through the event horizon is computed. Finally, the conclusions are given in the last section. Throughout the paper, we set $\hbar = c = G = 1$.

2. CHARGED VAIDYA MODEL

This section is devoted to the formulation of a spherically symmetric charged Vaidya model in the RN-like form using the procedure given in [19]. We skip the details of the procedure because they are already available and use only the required results. The spherically symmetric Vaidya-form metric is given by Eq. (2.34) in [19]:

$$ds^2 = -e^{\nu(t,r)}dt^2 + e^{\mu(t,r)}dr^2 + r^2 d\Omega^2, \qquad (1)$$

where

$$e^{\nu(t,r)} = \left(\frac{\dot{M}}{\chi(M)}\right)^2 e^{-\mu}, \quad e^{-\mu(t,r)} = 1 - \frac{2M}{r},$$

$$d\Omega^2 = d\theta^2 + \sin^2\theta d\phi^2,$$

$M(t,r)$ is a slowly varying mass function, and $\chi(M)$ depends on the details of the radiation. The corresponding field equations are [19]

$$\mu' = 8\pi r T_{rr} + \frac{1-e^{\mu}}{r}, \tag{2}$$

$$\nu' = 8\pi r e^{\mu-\nu} T_{tt} - \frac{1-e^{\mu}}{r}, \tag{3}$$

$$\dot{\mu} = 8\pi r T_{tr}, \tag{4}$$

$$1 - e^{-\mu} + \frac{1}{2} r e^{-\mu}(\mu' - \nu') - \frac{1}{2} r^2 R^{(0)} = = 8\pi T_{\theta\theta} = \frac{8\pi T_{\phi\phi}}{\sin^2\theta}, \tag{5}$$

where

$$R^{(0)} = -8\pi T^a{}_a = -\frac{2}{r^2}(1 - e^{-\mu}) + e^{-(\mu+\nu)/2} \times \times \left[\left(\dot{\mu} e^{(\mu-\nu)/2}\right)^{\cdot} - \left(\nu' e^{(\nu-\mu)/2}\right)'\right]. \tag{6}$$

The dot and prime respectively denote derivatives with respect to time and r. We note that Eqs. (2) and (4) represent the respective Hamiltonian and momentum constraints [20]. Equations (2) and (3) lead to

$$\frac{1}{2}(\mu' - \nu') = \frac{1-e^{\mu}}{r} \tag{7}$$

while Eqs. (5) and (6) yield

$$T_{rr} = e^{(\mu-\nu)} T_{tt}. \tag{8}$$

For the spherically symmetric Vaidya metric of form (1), we define $e^{-\mu(t,r)}$ by adding charge $Q(t,r)$ as follows:

$$e^{-\mu(t,r)} = 1 - \frac{2M(t,r)}{r} + \frac{Q^2(t,r)}{r^2}. \tag{9}$$

Using the procedure in [19], we can deduce from the field equations that

$$T^t{}_r e^{(\nu-\mu)/2} + T^t{}_t = 0. \tag{10}$$

Also, using Eqs. (2), (4), (8) and (10), we obtain

$$\mu' + \frac{e^{\mu} - 1}{r} + \dot{\mu} e^{(\mu-\nu)/2} = 0. \tag{11}$$

Inserting the value of e^{μ} from Eq. (9) gives

$$e^{\nu(t,r)} = \left(\frac{2Q\dot{Q}/r - 2\dot{M}}{2M' - 2QQ'/r + Q^2/r^2}\right)^2 \times \times \left(1 - \frac{2M}{r} + \frac{Q^2}{r^2}\right)^{-1}. \tag{12}$$

The corresponding form of the Vaidya solution [21] then becomes

$$ds^2 = -\left(\frac{2Q\dot{Q}/r - 2\dot{M}}{2M' - 2QQ'/r + Q^2/r^2}\right)^2 \times \times \left(1 - \frac{2M}{r} + \frac{Q^2}{r^2}\right)^{-1} dt^2 + + \left(1 - \frac{2M}{r} + \frac{Q^2}{r^2}\right)^{-1} dr^2 + r^2 d\Omega^2. \tag{13}$$

This is the spherically symmetric charged Vaidya model.

We now transform this metric to the RN-like form. For this, we write Eq. (12) in the form

$$e^{(\nu-\mu)/2} = \frac{r(2Q\dot{Q} - 2r\dot{M})}{2r^2M' - 2rQQ' + Q^2}. \tag{14}$$

Differentiating Eq. (14) with respect to r and using Eq. (7) yields

$$\frac{2Mr - Q^2}{r^2 - 2Mr + Q^2}[(Q\dot{Q} - r\dot{M})(2r^2M' - 2rQQ' + Q^2)] = = (2r^2M' - 2rQQ' + Q^2)(rQ\dot{Q}' + rQ'\dot{Q} + Q\dot{Q} - r^2\dot{M}' - -2\dot{M}r) - (2rQ\dot{Q} - 2r^2\dot{M})(r^2M'' + 2M'r - rQQ'' - rQ'^2)$$

which can also be written as

$$\frac{\left[\left(2M' - \frac{2QQ'}{r} + \frac{Q^2}{r^2}\right)\left(1 - \frac{2M}{r} + \frac{Q^2}{r^2}\right)\right]^{\cdot}}{\left[\left(2M' - \frac{2QQ'}{r} + \frac{Q^2}{r^2}\right)\left(1 - \frac{2M}{r} + \frac{Q^2}{r^2}\right)\right]'} = = \frac{\left(2M - \frac{Q^2}{r}\right)^{\cdot}}{\left(2M - \frac{Q^2}{r}\right)'}. \tag{15}$$

This has the solution

$$\left(2M' - \frac{2QQ'}{r} + \frac{Q^2}{r^2}\right)\left(1 - \frac{2M}{r} + \frac{Q^2}{r^2}\right) = = \chi(M, Q), \tag{16}$$

where $\chi(M,Q)\geq 0$. With the help of this equation, we can write Eq. (12) as

$$e^{\nu(t,r)}=e^{2\Psi(t,r)}\left(1-\frac{2M(t,r)}{r}+\frac{Q^2(t,r)}{r^2}\right), \qquad (17)$$

where

$$e^{2\Psi(t,r)}=\left(\frac{-2Q\dot{Q}/r+2\dot{M}}{\chi(M,Q)}\right)^2.$$

Consequently, the line element in (1) becomes

$$ds^2=-e^{2\Psi(t,r)}\left(1-\frac{2M(t,r)}{r}+\frac{Q^2(t,r)}{r^2}\right)dt^2+ \\ +\left(1-\frac{2M(t,r)}{r}+\frac{Q^2(t,r)}{r^2}\right)^{-1}dr^2+r^2d\Omega^2. \qquad (18)$$

This is the required spherically symmetric charged Vaidya model in the RN-like form. For a specific choice

$$\chi(M,Q)=-\left(-\frac{2Q\dot{Q}}{r}+2\dot{M}\right),$$

$\Psi(t,r)$ vanishes and hence (18) reduces to the simple RN-like form

$$ds^2=-F(t,r)\,dt^2+F^{-1}(t,r)\,dr^2+r^2d\Omega^2, \qquad (19)$$

where

$$F=1-\frac{2M(t,r)}{r}+\frac{Q^2(t,r)}{r^2}.$$

3. NONCOMMUTATIVE BLACK HOLE

Here, we develop a noncommutative form of the RN-like Vaidya metric in (19) by using the formalism of coordinate coherent states [18]. The mass/energy and charge distribution can be written as the following smeared delta functions ρ [17, 18]:

$$\rho_{matt}(t,r)=\frac{M}{(4\pi\sigma)^{3/2}}e^{-r^2/4\sigma}, \qquad (20)$$

$$\rho_{el}(t,r)=\frac{Q}{(4\pi\sigma)^{3/2}}e^{-r^2/4\sigma}, \qquad (21)$$

where σ is the noncommutative factor. The energy–momentum tensor for self-gravitating and anisotropic fluid source is given by

$$T_a{}^b=\begin{pmatrix} T_t{}^t & T_t{}^r & 0 & 0\\ T_r{}^t & T_r{}^r & 0 & 0\\ 0 & 0 & T_\theta{}^\theta & 0\\ 0 & 0 & 0 & T_\phi{}^\phi\end{pmatrix}. \qquad (22)$$

Here, we take

$$T_t{}^t=-(\rho_{matt}+\rho_{el})=T_r{}^r.$$

The corresponding field equations become

$$F'r+F+8\pi r^2(\rho_{matt}+\rho_{el})-1=0, \qquad (23)$$

$$\dot{F}-8\pi rF^2T_t{}^r=0, \qquad (24)$$

$$rF''F^3-2r\dot{F}^2+r\ddot{F}F+2F^3F'-16\pi rF^3T_\theta{}^\theta=0, \qquad (25)$$

$$T_t{}^r=T_r{}^t,\quad T_\phi{}^\phi=T_\theta{}^\theta. \qquad (26)$$

The conservation of the energy–momentum tensor,

$$T_a{}^b{}_{;b}=0,$$

yields

$$\partial_tT_t{}^t+\partial_rT_r{}^r+\frac{1}{2}g^{tt}\partial_rg_{tt}(T_r{}^r-T_t{}^t)- \\ -\frac{1}{2}g^{rr}\partial_tg_{rr}(T_r{}^r-T_t{}^t)+ \\ +g^{\theta\theta}\partial_rg_{\theta\theta}(T_r{}^r-T_\theta{}^\theta)=0$$

which leads to

$$\partial_tT_t{}^t+\partial_rT_t{}^t+g^{\theta\theta}\partial_rg_{\theta\theta}(T_t{}^t-T_\theta{}^\theta)=0.$$

Substituting, we obtain

$$T_\theta{}^\theta=(\rho_{matt}+\rho_{el})\times \\ \times\left(\frac{-r(\dot{M}+\dot{Q}+M'+Q')}{2(M+Q)}+\frac{r^2}{4\sigma}-1\right). \qquad (27)$$

We now consider the perfect fluid condition at large distances to determine the mass and charge functions. For this, we take isotropic pressure terms, i. e., $T_r{}^r=T_\theta{}^\theta$, and the above equation then yields

$$M+Q=C\exp\left[\frac{t^2}{4\sigma}+\frac{t(r-t)}{2\sigma}\right], \qquad (28)$$

where $C(r-t)$ is an integration function, which can be defined as

$$C(r-t)=M_I- \\ -Q_I^2\left[\varepsilon^2\left(\frac{r-t}{2\sqrt{\sigma}}\right)-\frac{1}{\sqrt{\pi}}\left(\frac{r-t}{\sqrt{2\sigma}}\right)\varepsilon\left(\frac{r-t}{\sqrt{2\sigma}}\right)\right]\times \\ \times\left[2r\left[\varepsilon\left(\frac{r-t}{2\sqrt{\sigma}}\right)\left(1+\frac{t^2}{2\sigma}\right)-\frac{r}{\sqrt{\pi\sigma}}\times\right.\right. \\ \left.\left.\times\exp\left(-\frac{(r-t)^2}{4\sigma}\right)\left(1+\frac{t}{r}\right)\right]\right]^{-1}. \qquad (29)$$

Here, M_I and Q_I are the initial BH mass and charge, and the Gauss error function is defined as

$$\varepsilon(x) \equiv \frac{2}{\sqrt{\pi}} \int_0^x e^{-p^2} dp.$$

Using Eq. (28) in (23), we obtain

$$F(t,r) = 1 - \frac{2M_\sigma(t,r)}{r} + \frac{Q_\sigma^2(t,r)}{r^2}, \qquad (30)$$

where the Gaussian smeared mass and charge distributions are

$$M_\sigma(t,r) = M_I \left[\varepsilon\left(\frac{r-t}{2\sqrt{\sigma}}\right)\left(1+\frac{t^2}{2\sigma}\right) - \right.$$
$$\left. - \frac{r\exp\left(-\frac{(r-t)^2}{4\sigma}\right)}{\sqrt{\pi\sigma}}\left(1+\frac{t}{r}\right)\right], \qquad (31)$$

$$Q_\sigma(t,r) = Q_I \left[\varepsilon^2\left(\frac{r-t}{2\sqrt{\sigma}}\right) - \right.$$
$$\left. - \frac{1}{\sqrt{\pi}}\left(\frac{r-t}{\sqrt{2\sigma}}\right)\varepsilon\left(\frac{r-t}{\sqrt{2\sigma}}\right)\right]^{1/2}.$$

This is the noncommutative form of (19).

The asymptotic form of (30) reduces to the RN metric for large distances at $t = 0$. Metric (30) characterizes the geometry of a noncommutativity-inspired RN-like Vaidya BH. The radiating behavior of such a modified BH can now be investigated by plotting g_{tt} for different values of M_I and Q_I. The coordinate noncommutativity leads to the existence of different causal structures, i. e., a nonextremal BH (with two horizons), an extremal BH (with one horizon), and charged massive droplet (with no horizon). Thus the noncommutative BH can shrink to the minimal nonzero mass with the minimal nonzero horizon radius.

4. HORIZON RADIUS AND BLACK HOLE EVAPORATION

Here, we investigate some features of the noncommutative metric in (30). First, we analyse the temporal component $g_{tt} = F(t,r)$ in the form of graphs versus the horizon radius $r/\sqrt{\sigma}$. The Table [18] provides values of the minimal nonzero mass as well as horizon radius with increasing time for an extremal BH. This shows that the minimal nonzero mass decreases whereas the minimal nonzero horizon radius increases with time, indicating that a micro BH evaporates completely, i. e., $M_0 \to 0$ for $t/\sqrt{\sigma} \gg 1$. Consequently, the concept of a BH remnant does not exist. The graphs of F are drawn for the following three cases: $M_I > M_0$, $M_I = M_0$, $M_I < M_0$.

Table. Extremal black hole

Time, t	Minimal nonzero mass, M_0 (appr.)	Minimal nonzero horizon radius, r_0 (appr.)
0	$1.90\sqrt{\sigma}$	$3.02\sqrt{\sigma}$
$1.00\sqrt{\sigma}$	$1.68\sqrt{\sigma}$	$4.49\sqrt{\sigma}$
$2.00\sqrt{\sigma}$	$0.99\sqrt{\sigma}$	$5.34\sqrt{\sigma}$
$3.00\sqrt{\sigma}$	$0.62\sqrt{\sigma}$	$6.14\sqrt{\sigma}$
$4.00\sqrt{\sigma}$	$0.43\sqrt{\sigma}$	$7.18\sqrt{\sigma}$
$5.00\sqrt{\sigma}$	$0.32\sqrt{\sigma}$	$8.32\sqrt{\sigma}$
$10.00\sqrt{\sigma}$	$0.13\sqrt{\sigma}$	$13.27\sqrt{\sigma}$
$100.00\sqrt{\sigma}$	$0.01\sqrt{\sigma}$	$105.05\sqrt{\sigma}$
$\to\infty$	$\to 0$	$\to\infty$

In the first case, the graphs of F are shown in Fig. 1. There, we choose different values of time $t/\sqrt{\sigma}$ with $M_I > M_0$ and fixed $M_I/\sqrt{\sigma}$ (i. e., $M_I = 3.00\sqrt{\sigma}$). The curves are marked from top down on the right side for $t = 0$, $1.00\sqrt{\sigma}$, $2.00\sqrt{\sigma}$, $3.00\sqrt{\sigma}$, and $4.00\sqrt{\sigma}$. This demonstrates that the distance between the horizons increases with time. When $t \to \infty$, we have two different horizons for the three possibilities of the initial mass and initial charge, i. e.,

$$\frac{Q_I}{\sqrt{\sigma}} < \frac{M_I}{\sqrt{\sigma}}, \quad \frac{Q_I}{\sqrt{\sigma}} = \frac{M_I}{\sqrt{\sigma}}, \quad \frac{Q_I}{\sqrt{\sigma}} > \frac{M_I}{\sqrt{\sigma}}.$$

Figure 2 shows the graphs of F when $M_I = M_0$. These represent the possibility of an extremum structure with one degenerate event horizon in the presence of charge. The possibilities for $M_I/\sqrt{\sigma}$ and $Q_I/\sqrt{\sigma}$ are given as follows.

1) For $Q_I/\sqrt{\sigma} < M_I/\sqrt{\sigma}$, it is possible to have one degenerate event horizon (extremal BH) for all t.

2) For $Q_I/\sqrt{\sigma} = M_I/\sqrt{\sigma}$, there is one degenerate event horizon for $t > 2$.

3) For $Q_I/\sqrt{\sigma} > M_I/\sqrt{\sigma}$, it is impossible to have a degenerate event horizon for all t.

Figure 3 shows graphs of F in the case $M_I < M_0$ with $M_I = 0.40\sqrt{\sigma}$. For all the three possibilities of the

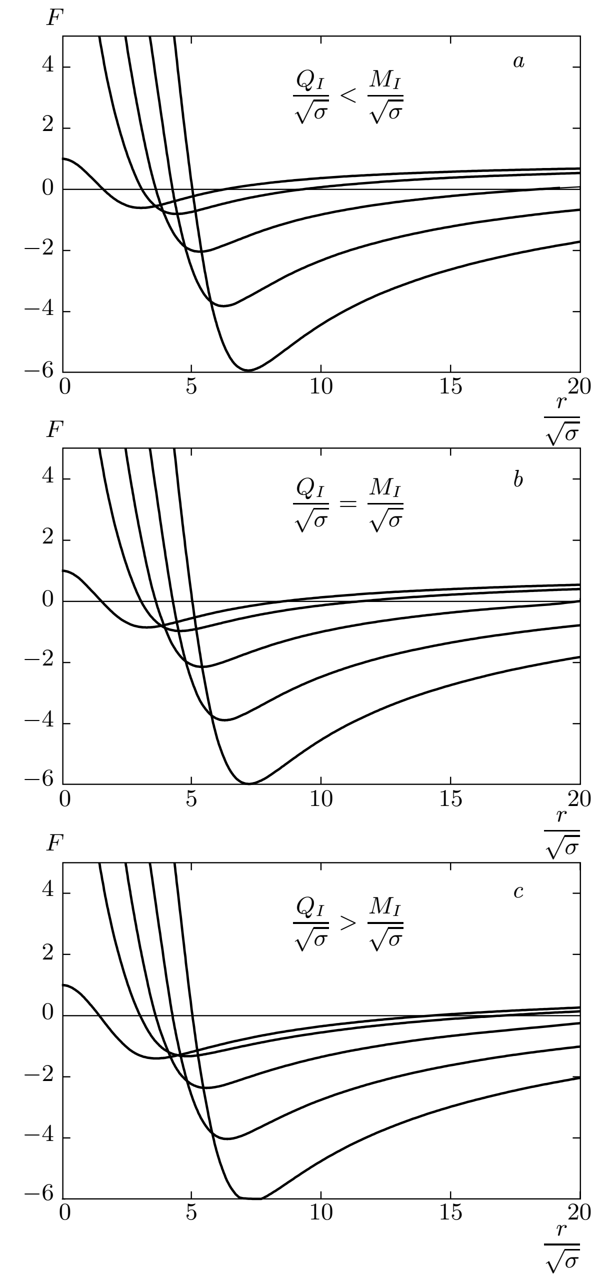

Fig. 1. a — $Q_I = 1.00\sqrt{\sigma} < M_I = 3.00\sqrt{\sigma}$; b — $Q_I = 3.00\sqrt{\sigma} = M_I$; c — $Q_I = 5.00\sqrt{\sigma} > M_I = 3.00\sqrt{\sigma}$

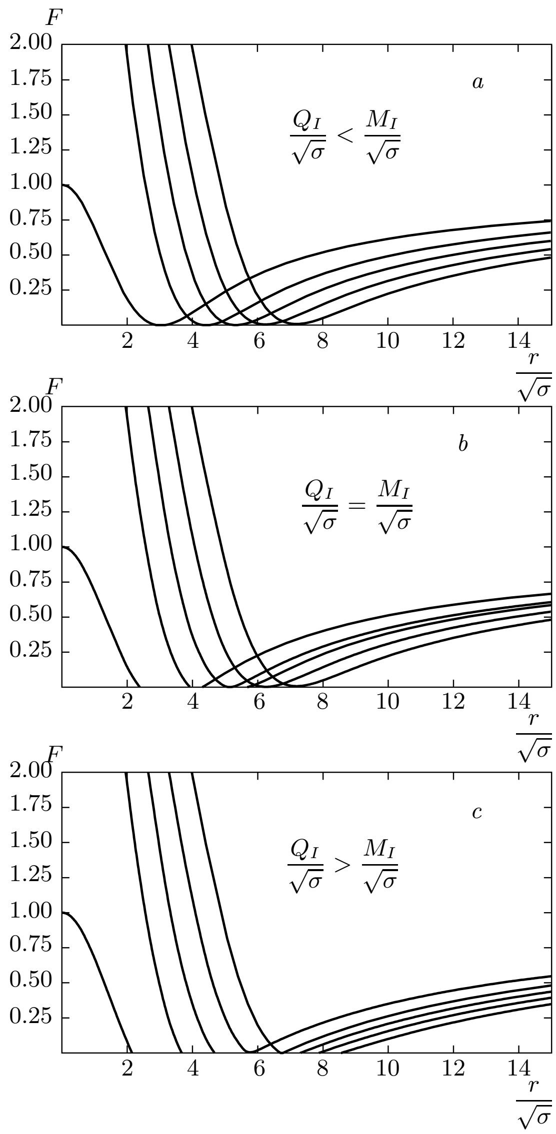

Fig. 2. a — $Q_I = 0.40\sqrt{\sigma} < M_I = M_0$; b — $Q_I = M_I = M_0$; c — $Q_I = 3.00\sqrt{\sigma} > M_I = M_0$

initial mass and charge, curves do not show any event horizon with the passage of time.

At $t = 0$, F in Eq. (30) takes the form

$$F(r) = 1 - \frac{2M_I}{r}\left[\varepsilon\left(\frac{r}{2\sqrt{\sigma}}\right) - \frac{r}{\sqrt{\pi\sigma}}e^{-r^2/4\sigma}\right] + \frac{{Q_I}^2}{r^2}\left[\varepsilon^2\left(\frac{r}{2\sqrt{\sigma}}\right) - \frac{1}{\sqrt{\pi}}\left(\frac{r}{\sqrt{2\sigma}}\right)\varepsilon\left(\frac{r}{\sqrt{2\sigma}}\right)\right]. \quad (32)$$

In the commutative limit, i. e., as $\sigma \to 0$, we have $\varepsilon(x) \to 1$, and hence F reduces to

$$F(r) = 1 - \frac{2M_I}{r} + \frac{{Q_I}^2}{r^2}. \quad (33)$$

The noncommutative form in Eq. (30) has a coordinate singularity at the event horizon r_H such that

$$r_H = M_\sigma(t, r_H) + \sqrt{M_\sigma^2(t, r_H) - Q_\sigma^2(t, r_H)}. \quad (34)$$

The analytic solution of this equation is not possible, but we can analyze the results graphically. For this,

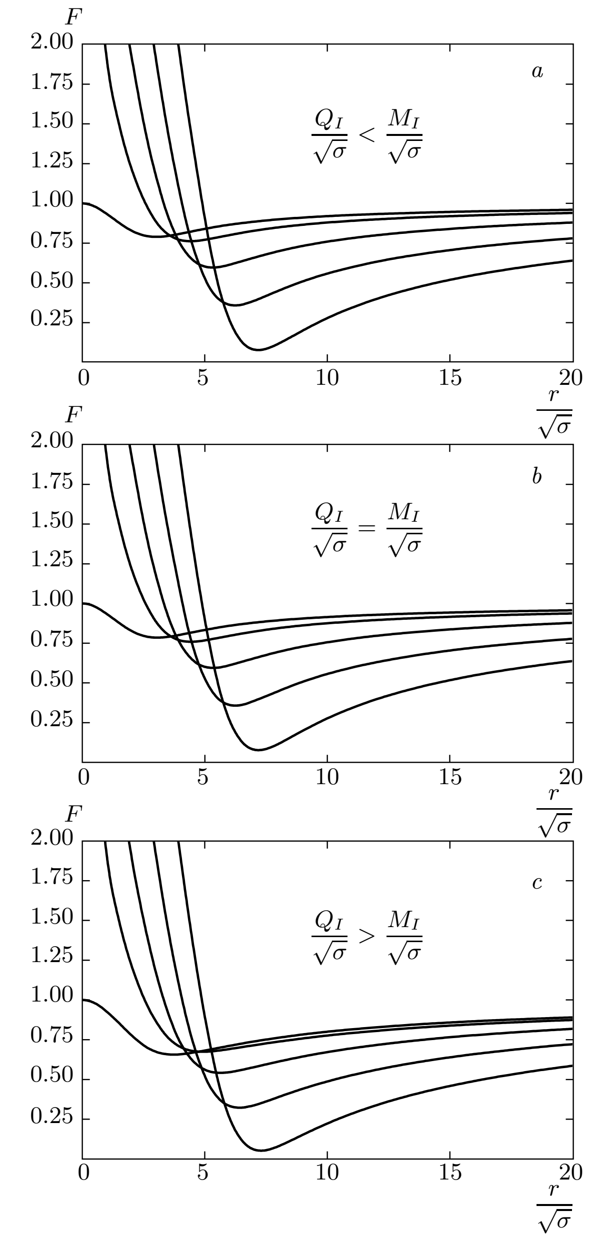

Fig. 3. a — $Q_I = 0.10\sqrt{\sigma} < M_I$; b — $Q_I = M_I$; c — $Q_I = 2.00\sqrt{\sigma} > M_I$

we substitute the values of M_σ and Q_σ from Eq. (31) in (34) and obtain

$$r_H^2 - 2r_H M_I \left[\varepsilon\left(\frac{r_H - t}{2\sqrt{\sigma}}\right)\left(1 + \frac{t^2}{2\sigma}\right) - \right.$$
$$\left. - \frac{r_H}{\sqrt{\sigma\pi}} \exp\left(-\frac{(r_H - t)^2}{4\sigma}\right)\left(1 + \frac{t}{r_H}\right)\right] =$$
$$= -Q_I^2 \left[\varepsilon^2\left(\frac{r_H - t}{2\sqrt{\sigma}}\right) - \frac{r_H - t}{\sqrt{2\sigma\pi}}\varepsilon\left(\frac{r_H - t}{\sqrt{2\sigma}}\right)\right]. \quad (35)$$

The graphical representation of this equation, shown in Fig. 4, is consistent with the Table. The initial mass (greater than the remnant mass) yields three possible causal structures depending on different values of the initial charge and the horizon radius with the passage of time.

We can summarize the behavior as follows.

1) For $Q_I/\sqrt{\sigma} < M_I/\sqrt{\sigma}$, $M_I/\sqrt{\sigma} \to 0$ as $Q_I/\sqrt{\sigma} \to \infty$ and $r_H/\sqrt{\sigma} \to \infty$.

In this case, figures show the stable phase of the BH. As times pases, the BH starts evaporation (due to charge), its mass reduces and approaches to zero for all horizon radii.

2) For $Q_I/\sqrt{\sigma} = M_I/\sqrt{\sigma}$, $M_I/\sqrt{\sigma} \to 0$ for all $r_H/\sqrt{\sigma}$ and $Q_I/\sqrt{\sigma}$ at large times.

Here, we see the initial stage of the BH evaporation in the figures. The black hole mass exhibits constant behavior (with the passage of time) for a small range of the horizon radius indicating no effect of charge. For large radius, due to effect of charge, the BH mass tends to zero for all horizon radii.

3) For $Q_I/\sqrt{\sigma} > \frac{M_I}{\sqrt{\sigma}}$, $M_I/\sqrt{\sigma} \to 0$ as $Q_I/\sqrt{\sigma} \to 0$ and $r_H/\sqrt{\sigma} \to \infty$.

This case yields the final stage of the BH evaporation. As time progresses, the BH evaporates completely, i. e., its mass and hence temperature tend to zero for all horizon radii.

These results imply the BH evaporation, which indicates the instability of the BH due to charge, and hence the BH must include a naked singularity. The total evaporation of the BH is possible when we consider a time-dependent BH mass [1, 22].

5. HAWKING RADIATION AS TUNNELING

In this section, we examine the radiation spectrum of an RN-like noncommutative BH by quantum tunneling [4]. The tunneling is a process where a charged particle moves in dynamical geometry and passes through the horizon without any singularity. It provides the emission rate of tunneled particle and depends on the key idea of energy conservation. The mass of the BH decreases appropriately when the virtual particle is emitted. This leads to a nonzero tunneling amplitude, which satisfies the original Hawking calculation [23]. In this process, the coordinate system used to eliminate coordinate singularity at the horizon is known as the Painlevé coordinate system [24]. The Painlevé time coordinate transformation is defined as

$$dt \to dt - \frac{\sqrt{1 - F(t,r)}}{F(t,r)}\, dr. \quad (36)$$

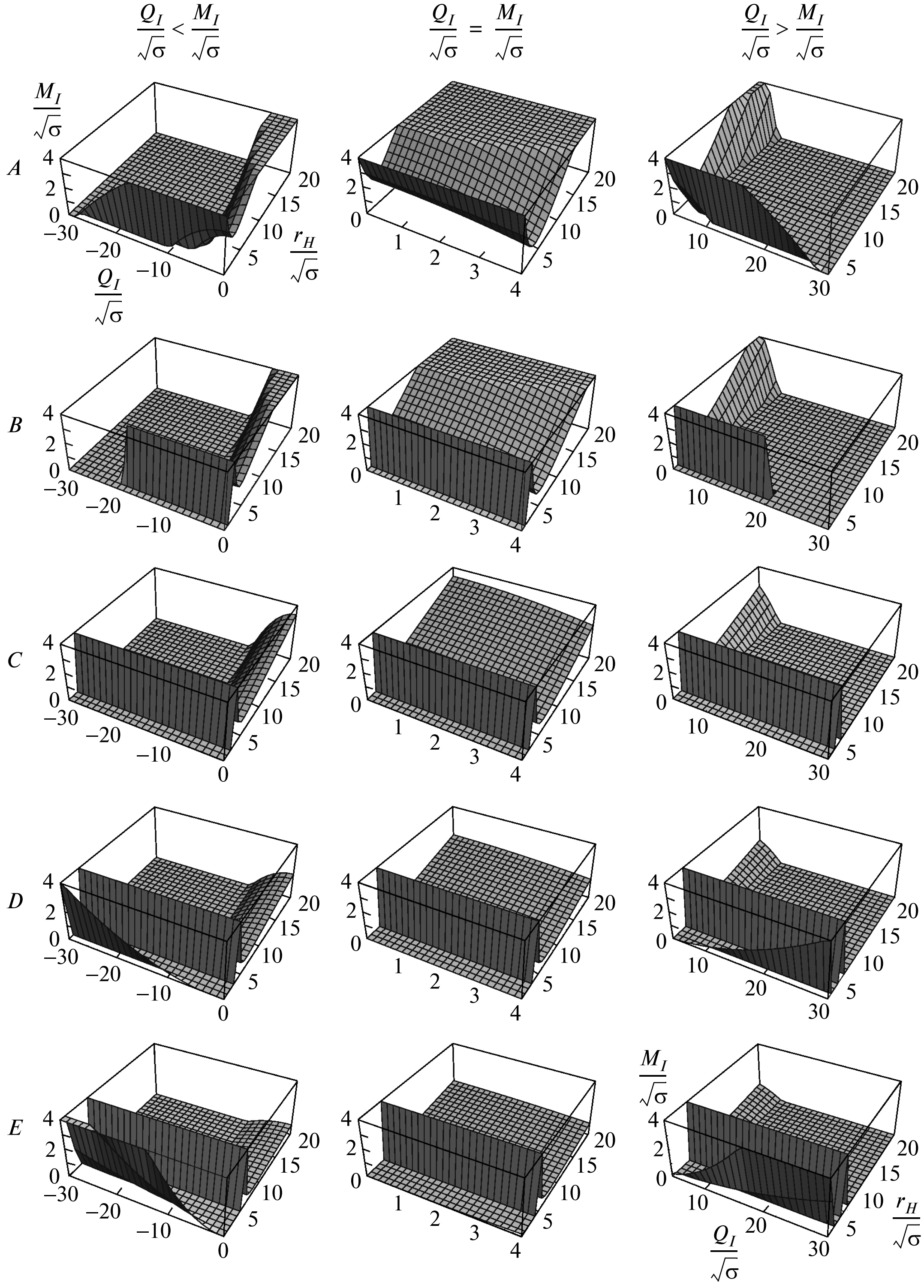

Fig. 4. A — $t = 0$; B — $t = 1.00\sqrt{\sigma}$; C — $t = 2.00\sqrt{\sigma}$; D — $t = 3.00\sqrt{\sigma}$; E — $t = 4.00\sqrt{\sigma}$; F — $t = 5.00\sqrt{\sigma}$; G — $t = 10.00\sqrt{\sigma}$; H — $t = 100.00\sqrt{\sigma}$

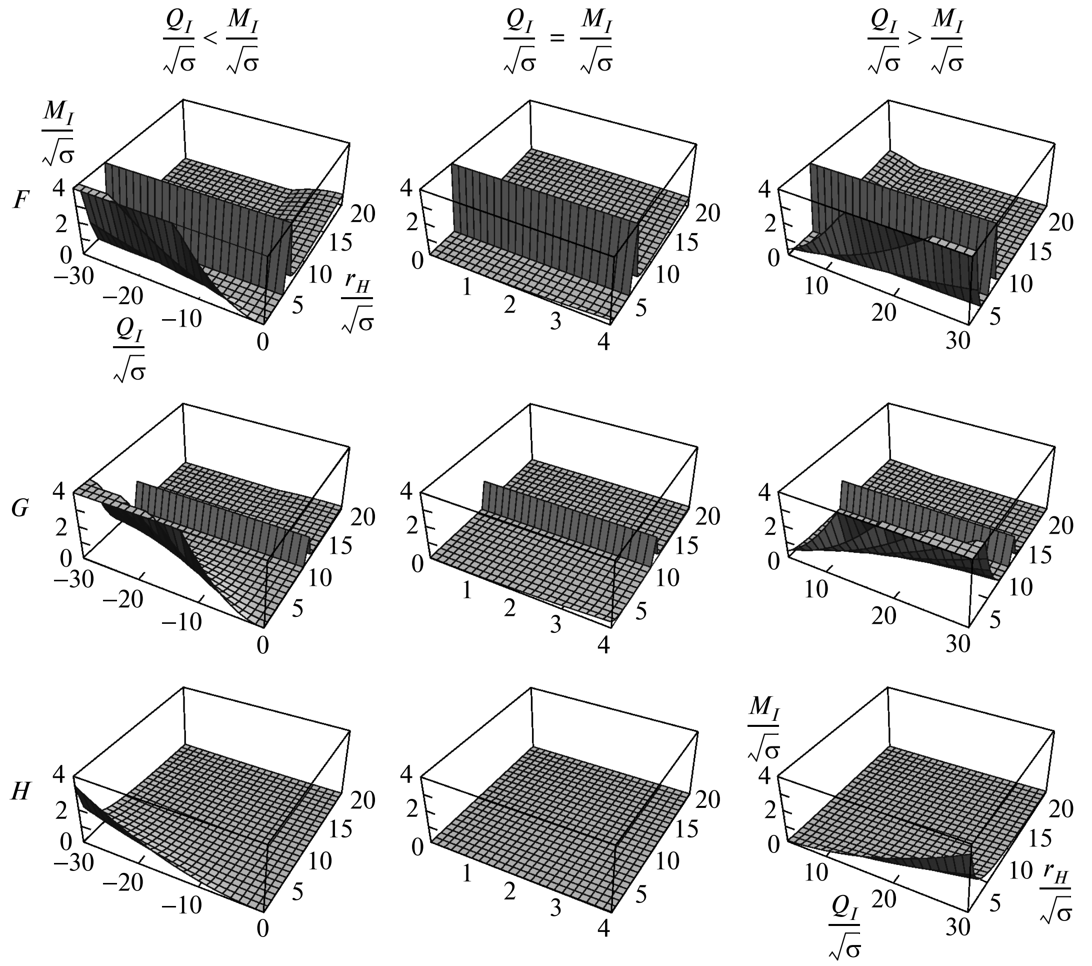

Fig. 4

Using this transformation, the corresponding spacetime in Eq. (19) can be written as

$$
\begin{aligned}
ds^2 &= -F(t,r)\,dt^2 + 2\sqrt{1-F(t,r)}dt\,dr + \\
&\qquad + dr^2 + r^2 d\Omega^2, \\
ds^2 &= -\left(1 - \frac{2M_\sigma(t,r)}{r} + \frac{Q_\sigma^2(t,r)}{r^2}\right) dt^2 + \\
&\quad + 2\sqrt{\frac{2M_\sigma(t,r)}{r} - \frac{Q_\sigma^2(t,r)}{r^2}}\,dt\,dr + dr^2 + r^2 d\Omega^2.
\end{aligned}
\tag{37}
$$

The outgoing motion (radial null geodesics, $ds^2 = d\Omega^2 = 0$) of massless particles takes the form

$$
\frac{dr}{dt} = 1 - \sqrt{1 - F(t,r)}. \tag{38}
$$

For an approximate value of $F(t,r)$ (short distances in a neighborhood of the BH horizon), we expand $F(t,r)$ up to the first order using the Taylor series, i. e.,

$$
\begin{aligned}
F(t,r)|_t &= F(t,r_H)|_t + F'(t,r_H)|_t(r - r_H) + \\
&\quad + O((r - r_H)^2)|_t.
\end{aligned}
\tag{39}
$$

Consequently, Eq. (38) becomes

$$
\frac{dr}{dt} \approx \frac{1}{2}F'(t,r_H)(r - r_H) \approx \kappa(M_I, Q_I)(r - r_H), \tag{40}
$$

where

$$
\kappa(M_I, Q_I) \approx \frac{1}{2}F'(t,r_H)
$$

is the surface gravity.

We now calculate the Hawking temperature of the RN-like BH. There are semiclassical methods to derive the Hawking temperature for the Vaidya BH [25]. From

$$
T_H = \frac{\kappa}{2\pi} = \frac{1}{4\pi}F'(t,r_H)|_t,
$$

it follows that

$$T_H = \frac{1}{4\pi} \times \left[-2M \left\{ \left(1 + \frac{t^2}{2\sigma}\right) \left(\frac{\exp\left(-\frac{(r_H - t)^2}{4\sigma}\right)}{r_H\sqrt{\pi\sigma}} - \frac{\varepsilon\left(\frac{r_H - t}{2\sqrt{\sigma}}\right)}{r_H^2} \right) - \frac{\exp\left(-\frac{(r_H - t)^2}{4\sigma}\right)}{\sqrt{\pi\sigma}} \left(-\frac{t}{r_H^2} - \frac{r_H - \frac{t^2}{r_H}}{2\sigma} \right) \right\} + Q^2 \left\{ \left(\frac{2\exp\left(-\frac{(r_H - t)^2}{4\sigma}\right)}{r_H^2\sqrt{\pi\sigma}} \times \varepsilon\left(\frac{r_H - t}{2\sqrt{\sigma}}\right) - \frac{2}{r_H^3}\varepsilon^2\left(\frac{r_H - t}{2\sqrt{\sigma}}\right) \right) - \frac{1}{\sqrt{2\pi\sigma}} \left(\left(\frac{1}{r_H} - \frac{t}{r_H^2}\right) \frac{\sqrt{2\exp\left(-\frac{(r_H - t)^2}{4\sigma}\right)}}{\sqrt{\pi\sigma}} + \varepsilon\left(\frac{r_H - t}{\sqrt{2\sigma}}\right)\left(-\frac{1}{r_H^2} - \frac{2t}{r_H^3}\right) \right) \right\} \right]. \quad (41)$$

For $t = 0 = Q_I$, this reduces to the Hawking temperature of the noncommutative Schwarzschild case [9].

Figure 5 shows the behavior of the Hawking temperature $T_H\sqrt{\sigma}$ versus horizon radius $r_H/\sqrt{\sigma}$ for fixed $M_I = 3.00\sqrt{\sigma}$. When the BH evaporates, there is no radiation and hence the temperature tends to zero. The graphs turn out to be smooth at the final stage of the BH evaporation. This can also be explained as follows. After the temperature reaches a maximum definite value at the minimal nonzero value of the horizon radius r_0, then it starts decreasing to the absolute zero and results in the mass tending to zero. For all the three possibilities of $M_I/\sqrt{\sigma}$ and $Q_I/\sqrt{\sigma}$, i.e.,

$$\frac{Q_I}{\sqrt{\sigma}} < \frac{M_I}{\sqrt{\sigma}}, \quad \frac{Q_I}{\sqrt{\sigma}} = \frac{M_I}{\sqrt{\sigma}}, \quad \frac{Q_I}{\sqrt{\sigma}} > \frac{M_I}{\sqrt{\sigma}},$$

the graphs of the Hawking temperature give the following behavior.

1) For $Q_I/\sqrt{\sigma} < M_I/\sqrt{\sigma}$, the behavior of curves is the same as in the Schwarzschild case [18].

2) For $Q_I/\sqrt{\sigma} = M_I/\sqrt{\sigma}$, the temperature increases at the minimal horizon radius.

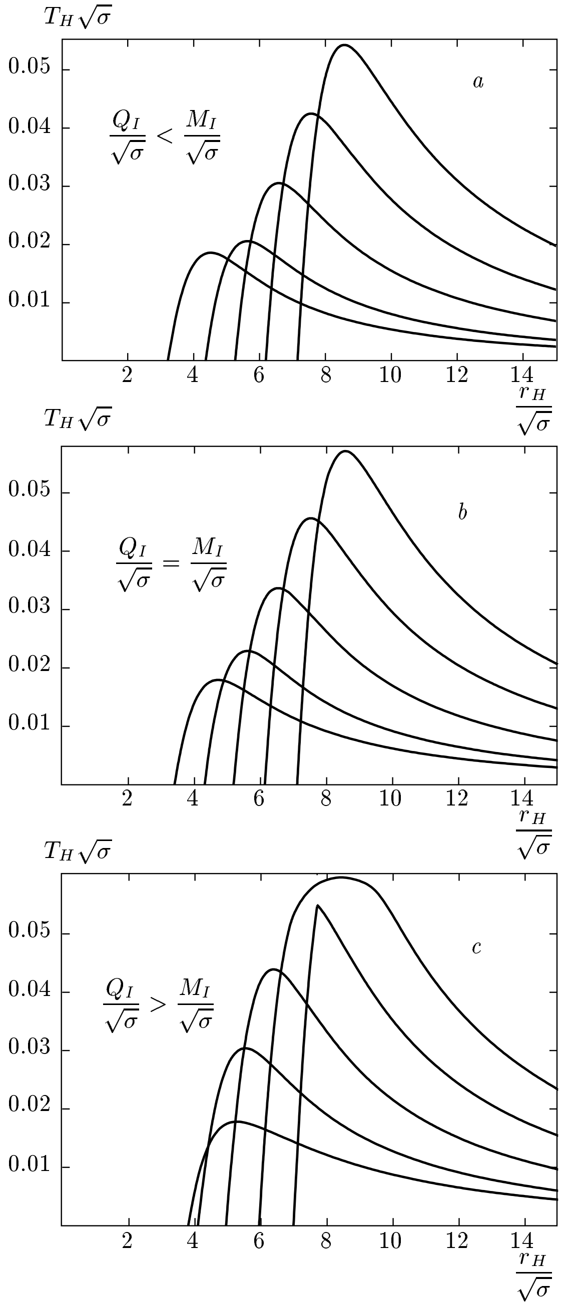

Fig. 5. a — $Q_I = 2.00\sqrt{\sigma} < M_I$; b — $Q_I = M_I$; c — $Q_I = 5.00\sqrt{\sigma} > M_I$

3) For $Q_I/\sqrt{\sigma} > M_I/\sqrt{\sigma}$, the horizon radius changes its position with increasing temperature.

We next discuss the effect of an electromagnetic field on the emission rate of charged particles tunneling through the quantum horizon of the BH. Here, we assume that an electromagnetic field is present outside the BH. The Lagrangian function for such a Maxwell gravity system can be defined as

$$L = L_{matt} + L_{el}, \tag{42}$$

where

$$L_{el} = -\frac{1}{4} F_{ab} F^{ab}$$

is the Maxwell Lagrangian function and F^{ab} is the Maxwell field tensor given by

$$F^{ab} = \partial^a \Phi^b - \partial^b \Phi^a, \tag{43}$$

where $\Phi_a = (\Phi, 0, 0, 0)$ is the electromagnetic 4-potential. The action and the rate of emission of a particle in the tunneling process are defined as [17]

$$I = \int_{t_{in}}^{t_{out}} (L_{matt} - p_\Phi \dot{\Phi})\, dt, \quad \Gamma \propto \exp(-2\,\mathrm{Im}\, I), \tag{44}$$

where p_Φ is the canonical momentum conjugate to Φ. In the tunneling process, the imaginary part of the amplitude for an s-wave, representing the outgoing positive-energy particles that cross the horizon outward from r_{in} to r_{out}, is given by

$$\mathrm{Im}\, I = \mathrm{Im} \int_{r_{in}}^{r_{out}} \left(p_r - \frac{p_\Phi \dot{\Phi}}{\dot{r}} \right) dr = \mathrm{Im} \int_{r_{in}}^{r_{out}} \left[\int_{(0,0)}^{(p_r, p_\Phi)} dp'_r - \frac{\dot{\Phi}}{\dot{r}} dp'_\Phi \right] dr. \tag{45}$$

The Hamilton equations of motion,

$$\begin{aligned} \frac{dr}{dt} &= \left.\frac{dH}{dp_r}\right|_{(r;\Phi,p_\Phi)} = \frac{d(M-E)}{dp_r} = -\frac{dE}{dp_r}, \\ \frac{d\Phi}{dt} &= \left.\frac{dH}{dp_\Phi}\right|_{(\Phi;r,p_r)} = -\Phi(Q-q)\frac{dq}{dp_\Phi}, \end{aligned} \tag{46}$$

provide the following relation of momentum and energy:

$$\mathrm{Im}\, I = \mathrm{Im} \int_{r_{in}}^{r_{out}} \left[\int_{(0,0)}^{(H,q)} \frac{dH'}{\dot{r}} + \frac{\Phi(Q-q')}{\dot{r}} dq' \right] dr. \tag{47}$$

In this process, particles and antiparticles can be respectively described as a positive and negative-energy solution of the wave equation. The BH accretes a small negative energy, which decreases its mass. Replacing M_I with $M_I - E$, Q_I with $Q_I - q$, and substituting Eq. (40) in (47), we obtain

$$\mathrm{Im}\, I = -\mathrm{Im} \int_{r_{in}}^{r_{out}} \left[\int_{(0,0)}^{(E,q)} \frac{dE'}{\kappa(M_I - E', Q_I - q')(r - r_H)} - \frac{\Phi(Q-q')\, dq'}{\kappa(M_I - E', Q_I - q')(r - r_H)} \right] dr. \tag{48}$$

This integral has a pole at the horizon r_H. To avoid this pole, we perform contour integration with the condition $r_{in} > r_{out}$ and obtain

$$\mathrm{Im}\, I = -\mathrm{Im} \left[\int_{(0,0)}^{(E,q)} \frac{dE'}{\kappa(M_I - E', Q_I - q')} - \frac{\Phi(Q-q')\, dq'}{\kappa(M_I - E', Q_I - q')} \right] \times \int_{r_{in}}^{r_{out}} \frac{dr}{r - r_H} = \pi \left[\int_{(0,0)}^{(E,q)} \frac{dE'}{\kappa(M_I - E', Q_I - q')} - \frac{\Phi(Q-q')\, dq'}{\kappa(M_I - E', Q_I - q')} \right]. \tag{49}$$

This shows that the particle emission rate is proportional to the surface gravity.

Using the first law of BH thermodynamics,

$$dM = T\, dS - \Phi\, dQ,$$

we write the imaginary part of the action $\mathrm{Im}\, I$ as [26]

$$\mathrm{Im}\, I = -\frac{1}{2} \int_{S_{NC}(M,Q)}^{S_{NC}(M-E,Q-q)} dS = -\frac{1}{2} \Delta S_{NC}, \tag{50}$$

where S_{NC} is the entropy of the noncommutative BH and ΔS_{NC} is the difference in BH entropies before and after the emission. At high energies, the tunneling amplitude (emission rate) depends on the final and initial number of microstates available to the system [27–30], implying that the emission rate is proportional to $\exp(\Delta S_{NC})$, i. e.,

$$\Gamma \propto \frac{\exp(S_{final})}{\exp(S_{initial})} = \exp(\Delta S_{NC}) = \exp\left[S_{NC}(M_I - E, Q_I - q) - S_{NC}(M_I, Q_I)\right]. \tag{51}$$

It follows that the emission spectrum cannot be precisely thermal. The modified noncommutative tunneling amplitude Γ can be computed if we know the analytic form of $\exp(\Delta S_{NC})$.

According to quantum theory, a BH is neither an absolute stationary state nor even a relative stationary state; it is an excited state of gravity. The vacuum state (excited state) generates spontaneous emission of virtual particles. The emission of charged particles by a BH is therefore physically equivalent to the spontaneous emission by an excited state [31].

6. SUMMARY

In this paper, we have derived a spherically symmetric charged Vaidya metric in the RN-like form and its noncommutative version. Noncommutativity implies a minimal nonzero mass that allows the existence of an event horizon. In order to investigate the BH horizon radius depending on time, mass, and charge, we have examined the behavior of $F(t,r)$ in the form of graphs, shown in Figs. 1–3 for three possible structures:

$$M_I > M_0, \quad M_I = M_0, \quad M_I < M_0.$$

These have further been discussed for three possibilities of the initial mass and the initial charge, i. e.,

$$\frac{Q_I}{\sqrt{\sigma}} < \frac{M_I}{\sqrt{\sigma}}, \quad \frac{Q_I}{\sqrt{\sigma}} = \frac{M_I}{\sqrt{\sigma}}, \quad \frac{Q_I}{\sqrt{\sigma}} > \frac{M_I}{\sqrt{\sigma}}.$$

The first case provides two different possible horizons. The second case represents the possibility of an extremum structure with one degenerate event horizon with time in the presence of a charge. In the last case, the curves do not indicate any event horizon.

In Fig. 4, the effects of charge on the BH evaporation are shown. The relations between mass and charge indicate three different stages of the BH mass and charge, which lead to the BH evaporation. Using the Table, we have found that the BH mass tends to zero as the horizon radius tends to infinity with time. This shows that the structure of a stable BH remnant having the capability of storing information is violated and information would disappear from our world. Hence, this leads to the evaporation of the BH and the final phase is a naked singularity. We have found that the BH evaporates completely in the large-time limit. We also see from these figures that the cases $Q_I/\sqrt{\sigma} < M_I/\sqrt{\sigma}$ and $Q_I/\sqrt{\sigma} > M_I/\sqrt{\sigma}$ indicate mutually reverse behavior.

The analysis of the Hawking temperature (Fig. 5) shows a behavior similar to that of the Schwarzschild spacetime. In the presence of a charge, the temperature attains a maximum position at the minimal nonzero horizon radius. As the horizon radius increases, the temperature vanishes, which corresponds to the BH evaporation, i. e., the mass tends to zero. Finally, we have discussed the Hawking radiation by using the Parikh–Wilczek tunneling process through the quantum horizon. The emission rate has been found consistent with the unitary theory. We have extended this analysis to compute the tunneling amplitude of charged massive particles from the RN-like Vaidya BH. It is mentioned here that corrections due to noncommutativity can be considered before the BH mass approaches the Planck mass.

It would be interesting to extend this work to the dyadosphere of the RN solution and the regular BH solutions in the noncommutative space. It would also be worthwhile to examine the behavior of thermodynamic quantities, evaporation of the BH remnant, and Hawking radiation as tunneling for these solutions.

We thank the Higher Education Commission, Islamabad, Pakistan for its financial support through the Indigenous Ph. D. 5000 Fellowship Program Batch-IV.

REFERENCES

1. S. W. Hawking, Comm. Math. Phys. **43**, 199 (1975).
2. S. W. Hawking, Phys. Rev. D **14**, 2460 (1976).
3. G. W. Gibbons and S. W. Hawking, Phys. Rev. D **15**, 2752 (1977).
4. M. K. Parikh and F. Wilczek, Phys. Rev. Lett. **85**, 5042 (2000).
5. T. Pilling, Phys. Lett. B **660**, 402 (2008).
6. V. Akhmedova et al., Phys. Lett. B **666**, 269 (2008).
7. S. Alexeyev, Class. Quantum Grav. **19**, 4431 (2002).
8. A. Smailagic and E. Spallucci, Phys. Rev. D **65**, 107701 (2002); J. Phys. A **35**, L363 (2002); J. Phys. A **36**, L467, L517 (2003); J. Phys. A **37**, 7169 (2004).
9. P. Nicolini, A. Smailagic, and E. Spallucci, Phys. Lett. B **632**, 547 (2006); S. Ansoldi, P. Nicolini, A. Smailagic, and E. Spallucci, Phys. Lett. B **645**, 261 (2007); P. Nicolini, Int. J. Mod. Phys. A **24**, 1229 (2009).
10. F. Nasseri, Int. J. Mod. Phys. D **15**, 1113 (2006).
11. K. Nozari and B. Fazlpour, Mod. Phys. Lett. A **22**, 2917 (2007); Acta Physica Polonica **39**, 1363 (2008).
12. J. Preskill, arXiv:9209058; D. N. Page, Phys. Rev. Lett. **71**, 3743 (1993); C. R. Stephens, G. 't Hooft, and B. F. Whiting, Class. Quantum Grav. **11**, 621 (1994); A. Strominger, arXiv:9501071; T. Banks, Nucl. Phys. (Proc. Suppl.) **41**, 21 (1995); J. G. Russo, arXiv:0501132.

13. M. Sharif and W. Javed, J. Korean Phys. Soc. **57**, 217 (2010).

14. M. Sharif and W. Javed, Candian J. Phys. **89**, 1027 (2011).

15. S. H. Mehdipour, Commun. Theor. Phys. **52**, 865 (2009).

16. K. Nozari and S. H. Mehdipour, Class. Quantum Grav. **25**, 175015 (2008).

17. S. H. Mehdipour, Int. J. Mod. Phys. A **25**, 5543 (2010).

18. S. H. Mehdipour, Phys. Rev. D **81**, 124049 (2010).

19. A. N. St. J. Farley and P. D. D'Eath, Gen. Relativ. Gravit. **38**, 425 (2006).

20. C. W. Misner, K. S. Thorne, and J. A. Wheeler, *Gravitation*, Freeman (1973).

21. P. C. Vaidya, Proc. Indian Acad. Sci. A **33**, 264 (1951).

22. J. D. Bekenstein, Phys. Rev. D **7**, 2333 (1973).

23. H. W. Hamber, *Quantum Gravitation: The Feynman Path Integral Approach*, Springer-Verlag, Berlin, Heidelberg (2009).

24. P. Painlevé, Compt. Rend. Acad. Sci. **173**, 677 (1921).

25. H. M. Siahaan and Triyanta, Int. J. Mod. Phys. A **25**, 145 (2010); arXiv:0811.1132.

26. E. Keski-Vakkuri and P. Kraus, Nucl. Phys. B **491**, 249 (1997).

27. M. Arzano, A. J. M. Medved, and E. C. Vagenas, JHEP **09**, 037 (2005); A. J. M. Medved and E. C. Vagenas, Mod. Phys. Lett. A **20**, 1723 (2005).

28. R. Banerjee, B. R. Majhi, and S. Samanta, Phys. Rev. D **77**, 124035 (2008); R. Banerjee and B. R. Majhi, Phys. Lett. B **662**, 62 (2008); JHEP **06**, 095 (2008).

29. R. Banerjee, B. Chakraborty, S. Ghosh, P. Mukherjee, and S. Samanta, Found. Phys. **39**, 1297 (2009); R. Banerjee, B. R. Majhi, and S. K. Modak, Class. Quantum Grav. **26**, 085010 (2009).

30. S. Massar and R. Parentani, Nucl. Phys. B **575**, 333 (2000).

31. L. Fang and R. Ruffini, *Basic Concepts in Relativistic Astrophysics*, World Scientific, (1983).